Modern Pathology (2021) 34:490–501
https://doi.org/10.1038/s41379-020-00648-y

ARTICLE

# Characterization of *TP53*-wildtype tubo-ovarian high-grade serous carcinomas: rare exceptions to the binary classification of ovarian serous carcinoma

M. Herman Chui[1] · Amir Momeni Boroujeni[1] · Diana Mandelker[1] · Marc Ladanyi[1] · Robert A. Soslow[1]

Received: 19 May 2020 / Revised: 27 July 2020 / Accepted: 28 July 2020 / Published online: 15 August 2020


## Abstract

While *TP53* mutation is widely considered to be a defining feature of tubo-ovarian high-grade serous carcinoma (HGSC), rare *TP53*-mutation-negative cases have been reported. To gain further insight into this rare subset, a retrospective review was conducted on 25 *TP53*-wildtype tubo-ovarian HGSCs, constituting 2.5% of 987 HGSCs profiled by the MSK-IMPACT sequencing platform. Consistent with serous differentiation, positive staining for Pax8 and WT1 was present in virtually all *TP53*-wildtype HGSCs. Other characteristic features of HGSC, such as serous tubal intraepithelial carcinoma, or genetic alterations of *CCNE1* and *BRCA1/2* were identified in these tumors, furthering supporting their classification as *bona fide* HGSC, despite lacking *TP53* mutations. Overall, the level of chromosomal instability of *TP53*-wildtype HGSCs was intermediate between low-grade serous carcinoma (LGSC) and *TP53*-mutated HGSC. Morphologic assessment by observers blinded to mutation status revealed a significant subset of tumors with Grade 2 nuclear atypia (which exceeds the degree of atypia allowed for LGSC, but less than typically encountered for HGSC) combined with micropapillary features (6/19, 32%, chemotherapy-naive *TP53*-wildtype HGSCs compared to 0/21, 0%, *TP53*-mutated HGSCs; $p = 0.007$). Some *TP53*-wildtype HGSCs harbored driver mutations in *KRAS* ($n = 3$), *BRAF* ($n = 1$) or *NRAS* ($n = 2$). Overall, 10 (40%) cases had "LGSC-like" morphology (i.e., Grade 2 nuclear atypia and micropapillary features) and/or *RAS/RAF* mutation, and most of these showed a wildtype p53 pattern of expression by immunohistochemistry (7/9, 78%). The remaining *TP53*-wildtype HGSCs ($n = 15$, 60%) exhibited severe nuclear atypia (Grade 3) and were morphologically indistinguishable from conventional *TP53*-mutated HGSC. Despite lacking genetic alterations of *TP53*, these "usual HGSC-like" tumors often showed evidence of p53 dysfunction, including downregulation of expression ('null' or equivocal p53 staining in 9/14, 64%) or *MDM2* amplification ($n = 2$). Our results support the existence of *TP53*-wildtype HGSCs, which comprise a heterogeneous group of tumors which may arise via distinct pathogenic mechanisms.

## Introduction

The dualistic model of ovarian serous neoplasia separates high-grade and low-grade serous carcinoma (LGSC) into distinct entities, based on differences in clinical, morphologic, and molecular features [1]. High-grade serous carcinoma (HGSC) is the most common and aggressive form of ovarian cancer. Most cases are thought to originate from the distal fallopian tube, arising from a precursor lesion termed serous tubal intraepithelial carcinoma (STIC) [2, 3]. As implied by the diagnostic terminology, HGSC is characterized by severe ('high-grade') nuclear atypia and high mitotic rate, correlating at the molecular level with a high degree of chromosome instability [4]. Approximately 15–20% of patients with tubo-ovarian HGSC harbor germline mutations in *BRCA1* or *BRCA2*, and rare cases are associated with mutations in other genes involved in homologous recombination (e.g., *BRIP1*, *PALB2*, *RAD51C*), which account for up to an additional 6% of patients [4, 5]. Large-scale sequencing efforts have identified mutations in *TP53* in nearly all tubo-ovarian HGSCs [5]. In the Cancer Genome Atlas (TCGA) cohort, rare

**Supplementary information** The online version of this article (https://doi.org/10.1038/s41379-020-00648-y) contains supplementary material, which is available to authorized users.

✉ M. Herman Chui
dr.michaelherman.chui@gmail.com

[1] Department of Pathology, Memorial Sloan Kettering Cancer Center, New York, NY, United States

HGSCs lacking *TP53* mutations have been reported. However, subsequent independent review revealed that many of these were in fact, other entities that were misclassified as HGSC [6].

In contrast to HGSC, LGSC lacks *TP53* mutations and carries few mutations and copy number alterations [1, 7]. Approximately 60% of LGSCs harbor driver mutations in genes involved in RAS/MAPK signaling, namely, *KRAS*, *NRAS* and, less frequently, *BRAF* or *ERBB2*. Distinguishing LGSC from HGSC is based primarily on the degree of nuclear pleomorphism, with mitotic rate as a secondary criterion [4, 8]. While the pathogeneses of ovarian LGSC and HGSC generally proceed along distinct, non-overlapping pathways, low-grade serous tumors can occasionally transform into HGSC, a process that may involve, though not necessarily require, acquisition of *TP53* mutation [9–13].

In the present study, we conducted a retrospective query of over 1000 tubo-ovarian HGSCs, diagnosed at our institution and subjected to targeted next-generation sequencing using the Memorial Sloan Kettering-Integrated Mutational Profiling of Actionable Cancer Targets (MSK-IMPACT) platform, to identify *TP53*-wildtype cases. Here, we report the results of histomorphologic, immunophenotypic and molecular features of this rare subgroup of HGSCs that defy the binary classification of ovarian serous carcinoma.

## Materials and methods

### Patient cohort

This study was approved by our institutional review board. From July 2014 until January 2020, tumor mutational profiling was performed on 1017 patients with a pathologic diagnosis of fallopian tube or ovarian HGSC rendered at our institution, using MSK-IMPACT (See *Next-generation sequencing and analysis of somatic genetic alterations* for details and Fig. 1 for a flowchart of the case selection process). Somatic *TP53* mutation was reported in 962 cases. In 20 of the 55 cases reported as being "negative" for *TP53* mutation, MSK-IMPACT detected no somatic genetic alterations across the panel, or at most, a few low allelic frequency (<5%) variants (including a *TP53*-C135Y mutation detected at 2% variant allele frequency in 1 case). Slide review confirmed low tumor cellularity, and as expected, most of these patients ($n = 18$, 90%) were treated with neoadjuvant chemotherapy. Immunohistochemical staining was performed on 17 of the 20 cases, for which tissue was available, and demonstrated aberrant p53 staining in 88% [15/17; diffuse ($n = 9$), complete lossor 'null' pattern ($n = 6$)]. The inability to detect *TP53* genetic alterations in these tumors was therefore considered artefactual, rather than reflective of underlying biology. While

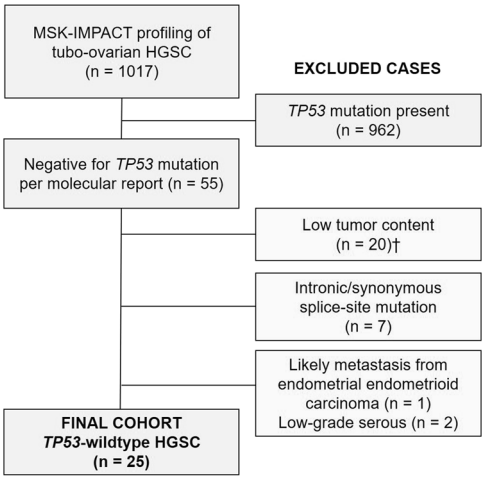


**Fig. 1 Flow diagram depicting case selection process.** †18/20 post-neoadjuvant chemotherapy; (15/17 with aberrant p53 staining pattern).

these cases were excluded from further analyses, they illustrate the practical utility of performing p53 immunohistochemistry to corroborate the diagnosis of HGSC in the clinical scenario of a negative sequencing result due to low tumor cellularity.

Re-review of the *TP53*-sequencing reads led to exclusion of 7 further cases with challenging and unusual *TP53* variants: specifically, an intronic variant, c. 375+5G>T ($n = 5$) and a known pathogenic variant resulting in a synonymous mutation, c.375G>A, pThr125= ($n = 1$), both of which were predicted to cause aberrant splicing of the gene; in the remaining case, there was a large deletion of exons 10 and 11 ($n = 1$).

Histologic re-review (see *Histomorphologic review and morphologic terminology* for details) led to exclusion of an ovarian carcinosarcoma with a high-grade serous component (harboring a *KRAS* mutation and *HER2* amplification) as the patient also had a concurrent endometrial carcinoma, and the ovarian tumor likely represented a metastasis. Another 2 cases re-classified as LGSC were also excluded. Following manual review of the sequencing data and histologic review, we arrived at a final cohort of 25 *TP53*-wildtype HGSCs.

For the final cohort of 25 patients deemed to have bona fide *TP53*-wildtype HGSC, the following information was extracted from the clinical records: age, stage of disease at presentation, treatment with neoadjuvant chemotherapy, prior history of a low-grade serous tumor (i.e. serous borderline tumor or LGSC), germline mutation testing results, and overall survival.

### Histomorphologic review and morphologic terminology

Representative slides of the 55 HGSCs initially reported as negative for *TP53* mutation and 35 consecutive *TP53*-

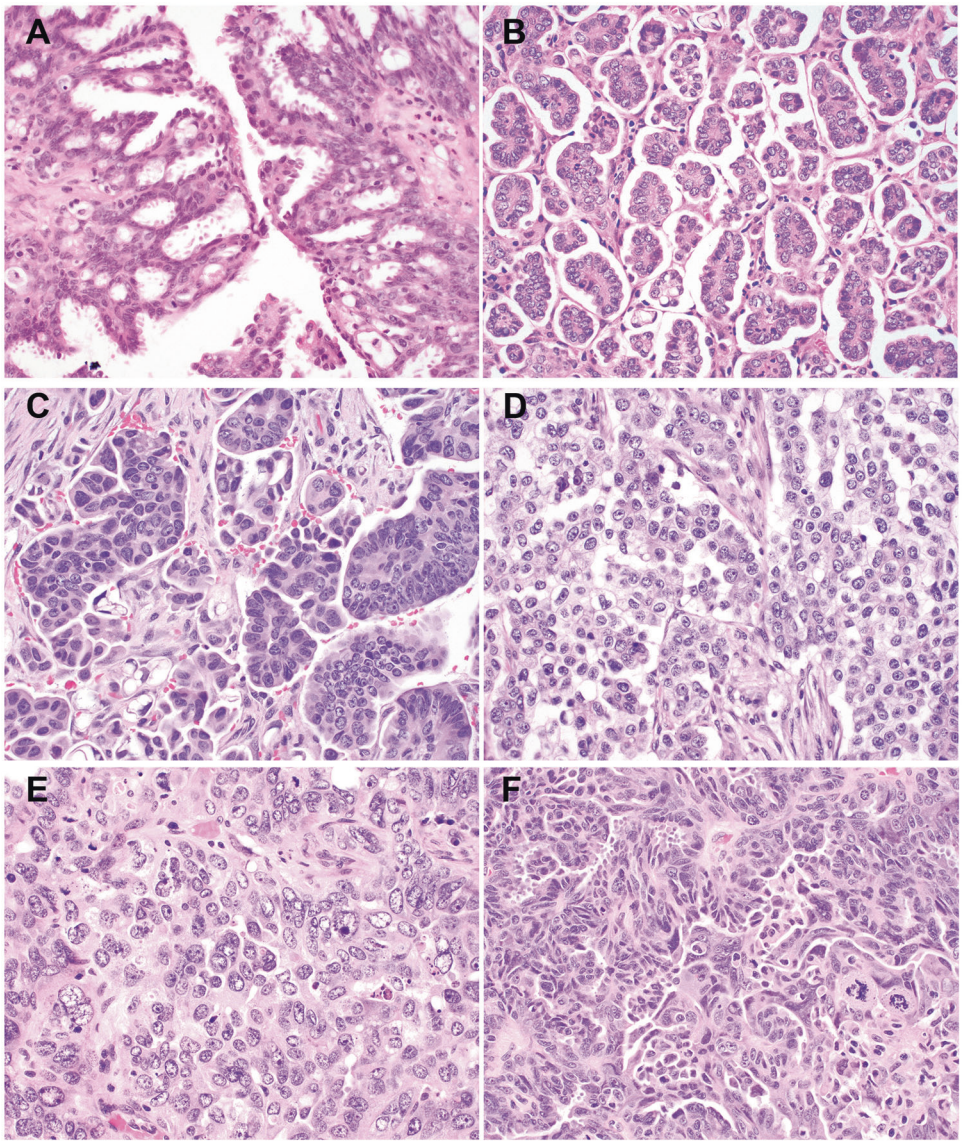


**Fig. 2 Nuclear grading and micropapillary features.** **a**, **b** Grade 1 nuclei from representative LGSCs. These tumors typically exhibit micropapillary features. **a** Micropapillae of length at least three times width, and some fusion of micropapillae resulting in cribiforming and **b** detached micropapillae, forming small solid nests within clefted spaces. **c**, **d** Grade 2 nuclear atypia from *TP53*-wildtype HGSCs with micropapillary features (Cases 2 and 8, respectively). **e**, **f** Grade 3 nuclear atypia from HGSC **e** with *TP53* mutation, and **f** from a *TP53*-wildtype HGSC (Case 17). All photomicrographs at ×400 magnification.

mutated HGSCs were reviewed by two gynecologic pathologists (MHC and RAS) blinded to all clinical and molecular information. Representative H&E-stained slides of tumor were selected and cases were randomly re-ordered and re-labeled for histologic review. Slide review was performed using a multi-head microscope with the diagnostic impression reached by consensus agreement using standard diagnostic criteria [4]; cases morphologically inconsistent with HGSC on re-review were excluded from further analysis. For each case, the following features were also assessed: degree of nuclear atypia, predominant architectural growth pattern and mitotic figures per 10 high-powered fields. At the time of unblinding, nuclear atypia, architectural pattern and mitotic counts were excluded for all tumors treated with chemotherapy (which was confirmed by review of the clinical record). For these morphologic features, statistical comparisons between groups were limited to chemotherapy-naive cases ($n = 19$ *TP53*-wildtype versus $n = 21$ *TP53*-mutated HGSCs). However, it should be noted that treated tumors were still included for other descriptive analyses. For 3 of the 6 patients treated with chemotherapy, slides of a pre-treatment specimen were retrieved, and morphologic review confirmed the diagnosis of HGSC (Supplementary Table S1).

Nuclear atypia was assessed using a 3-tiered grading system (Fig. 2a–e). Grade 1, or low-grade atypia, denoted uniform round or oval nuclei, while Grade 3, or high-grade nuclear atypia referred to large, hyperchromatic and pleomorphic nuclei with >3:1 size variation overall. Grade 2 designated enlarged and overlapping, but relatively uniform nuclei with <3:1 size variation, though focal high-grade nuclei (including large, bizarre forms) were allowed. Of note,

the presence of focal high-grade nuclei was a helpful morphologic finding supporting the diagnosis of HGSC rather than LGSC. Tumors with low-grade areas admixed with a high-grade component were also classified as Grade 2.

The predominant architectural growth pattern was classified as: solid, papillary, glandular, or micropapillary. The term "micropapillary" was used to denote papillary/pseudopapillary structures of length 3 times greater than width, but also encompassed the following variants: (1) cribiform growth, resulting from fusion of micropapillae, and (2) small solid cell nests or detached micropapillae within clefted spaces. Combination of different patterns was also noted.

After applying exclusion criteria to arrive at the final cohort of 25 cases of bona fide *TP53*-wildtype HGSC, available diagnostic slides of fallopian tube were reviewed for each of these cases by one pathologist (MHC) to assess for STIC or mucosal involvement by carcinoma.

### Immunohistochemistry

Immunohistochemical staining was performed on FFPE sections of tumor tissue, subject to tissue availability (23 of 25 cases), using the following markers/primary antibodies: p53 (clone D07, Ventana), WT1 (clone WT49, Leica), and Pax8 (clone BC12, Biocare). The staining pattern for p53 was assessed as wildtype, diffuse, null, cytoplasmic (mutant-type), or equivocal; WT1 and Pax8 stains were classified as positive or negative.

### Next-generation sequencing and analyses of somatic genetic alterations

Molecular genetic profiling was performed using MSK-IMPACT, a hybridization-capture-based next-generation-sequencing assay developed at our institution that provides full exon coverage from at least 410 known cancer genes (468 genes in the latest version), as previously described [14]. Germline testing was performed using the MSK-IMPACT germline gene panel covering 76 known cancer susceptibility genes. The MSK-IMPACT variant calling algorithm uses VARDICT and MUTECT and filters out non-somatic (i.e., germline) variants using matched normal DNA from peripheral blood. Silent variants, intronic variants (including splice site variants further than 3 bp from an exon), and variants with low variant allele frequency (<2%) are also filtered out. Therefore, manual review of the somatic variant calls and sequencing reads of the *TP53* gene was performed for all 55 cases of HGSC for which a *TP53* mutation was not reported, to identify any cases with unusual variants (with pathogenicity confirmed using ClinVar) or mutations occurring at low variant allele frequency. For somatic alterations in other cancer genes, only those annotated as Pathogenic or Likely Pathogenic are presented in this paper.

Fraction of genome altered, and total number of mutations were determined from MSK-IMPACT sequencing data from 20 *TP53*-wildtype HGSCs with high sequencing coverage (>500×) and adequate tumor content (>25% as estimated by histologic review) and from 58 LGSCs and 102 *TP53*-mutated HGSCs randomly selected from our institutional cohort. Breakpoint instability index was calculated using the modified Bayes Information Criterion, implemented in the *R* package WBS, on MSK-IMPACT segmentation files containing focal copy number data [15].

### Statistical analysis

For categorical data, comparisons between groups were analyzed by the Fisher exact test. Comparisons of ordinal data (i.e. measures of global genomic alterations) were performed using the Mann–Whitney *U* test. All statistical tests were two-tailed, with the threshold for statistical significance at $p < 0.05$.

## Results

### Identification of *TP53*-wildtype high-grade serous carcinomas and cohort characteristics

By applying stringent exclusion criteria (see "Methods" section for details), we identified 25 cases of bona fide *TP53*-wildtype HGSCs (Supplementary Table S1), representing 2.5% of 987 tubo-ovarian HGSCs, after adjusting for excluded cases. Consistent with serous differentiation, immunohistochemical staining demonstrated all *TP53*-wildtype HGSCs with available tissue to be positive for WT1 (23/23) and nearly all were positive for Pax8 (22/23). Figure 3 summarizes the clinical, pathologic and molecular features for each of these cases. The median age was 62 (range 37–78). Stage distribution was as follows: 1 (4%) Stage I, 12 (48%) Stage III, and 12 (48%) Stage IV. Six (24%) patients received neoadjuvant chemotherapy. Four (16%) patients had a prior history of serous borderline tumor ($n = 2$) or LGSC ($n = 2$). The median length of clinical follow-up was 44 months (range 4–130 months), with 5 (20%) alive without evidence of disease, 17 (68%) alive with disease, and 3 (12%) dead of disease at the time of last follow-up (Supplementary Table S1).

### Histomorphologic features of *TP53*-wildtype versus *TP53*-mutated HGSCs

Cytomorphologic and architectural features were assessed in *TP53*-mutant and *TP53*-wildtype tubo-ovarian HGSCs by

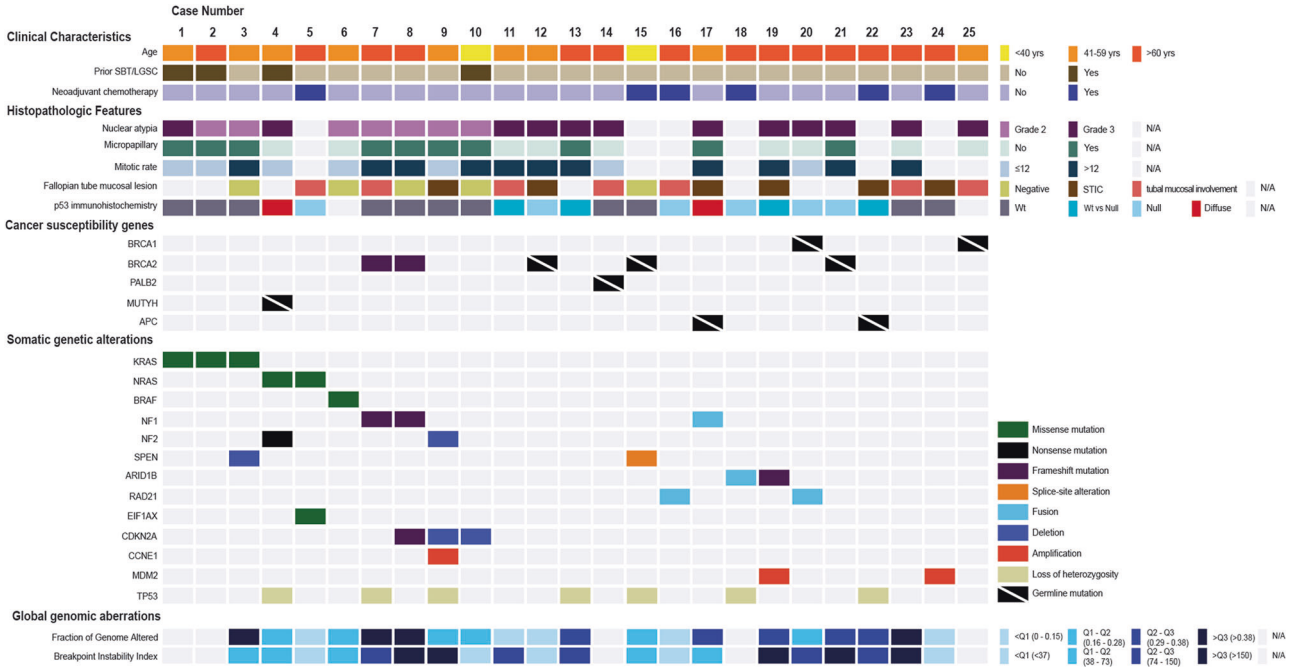


**Fig. 3 Clinical, pathologic, and molecular genetic features of 25 *TP53*-wildtype HGSCs.** SBT serous borderline tumor, LGSC low-grade serous carcinoma, STIC serous tubal intraepithelial carcinoma, Wt wildtype ('Wt versus Null' is equivocal), N/A not applicable. Note: certain tumor morphologic features were excluded for chemotherapy-treated cases.

**Table 1** Histomorphologic features of HGSCs stratified by *TP53* mutation status.

| | | Wildtype ($n = 19$) | Mutated ($n = 21$) | $p$ Value |
|---|---|---|---|---|
| Nuclear atypia | Grade 2 | 7 (37%) | 0 (0%) | 0.003 |
| | Grade 3 | 12 (63%) | 21 (100%) | |
| Micropapillary features[a] | Yes | 10 (53%) | 1 (5%) | 0.001 |
| | No | 9 (47%) | 20 (95%) | |
| Both Grade 2 nuclei and micropapillary features | Yes | 6 (32%) | 0 (0%) | 0.007 |
| | No | 13 (68%) | 21 (100%) | |
| Mitotic count (per 10 high-powered fields)[b] | ≤12 | 7/18 (39%) | 4 (19%) | 0.28 |
| | >12 | 11/18 (61%) | 17 (81%) | |

Only chemotherapy-naive cases included.

[a]Micropapillary features include any of the following as the predominant architecture pattern: (1) papillary/pseudopapillary structures of length 3 times greater than width, (2) cribiform structures resulting from fusion of micropapillae, and (3) small solid cell nests or detached micropapillae within clefted spaces.

[b]One case was excluded (Case 25), due to insufficient tissue for a formal mitotic count.

observers blinded to mutation status. Only chemotherapy-naive cases were included for comparisons between the two groups (Table 1). As expected, all *TP53*-mutated HGSCs ($n = 21$) showed severe nuclear atypia throughout, with predominant solid, papillary or glandular architecture, or a combination of patterns. This contrasted with a significantly lower proportion of nuclear Grade 3 *TP53*-wildtype tumors (12/19, 63%; $p = 0.003$), with the remainder categorized as Grade 2 (as defined in the "Methods" section; Figs. 2c, d and 4a–e). *TP53*-wildtype HGSCs were more likely to show micropapillary features (including cribiform or small solid nests within clefted spaces; 10/19, 53%, versus 1/21, 5%, of *TP53*-mutated HGSCs, $p = 0.001$). While often seen in conjunction with Grade 2 nuclear atypia, some nuclear Grade 3 *TP53*-wildtype tumors also showed micropapillary features ($n = 4$). The combination of Grade 2 nuclear atypia and micropapillary pattern was observed significantly more frequently in *TP53*-wildtype HGSCs compared to *TP53*-mutated HGSCs (6/19, 32%, versus 0/21, 0%; $p = 0.007$). There was no significant difference in the proportion of cases with low mitotic rates (≤12 per 10 high-powered fields) in *TP53*-wildtype compared to *TP53*-mutant HGSCs ($p = 0.28$).

## Morphologic and molecular subclassification of *TP53*-wildtype HGSC

It became clear from the histomorphologic and mutational data (See *Somatic driver gene mutations and copy number alterations* section for details), that *TP53*-wildtype HGSCs could be subclassified into two distinct groups (Fig. 5). By integrating morphologic and mutational data, we use the term, "LGSC-like" HGSC to describe *TP53*-wildtype HGSCs that have: (1) *KRAS*, *BRAF* or *NRAS* mutation, and/or (2) micropapillary features in conjunction with Grade 2 nuclear atypia (whereby the higher degree of atypia precludes classification as LGSC

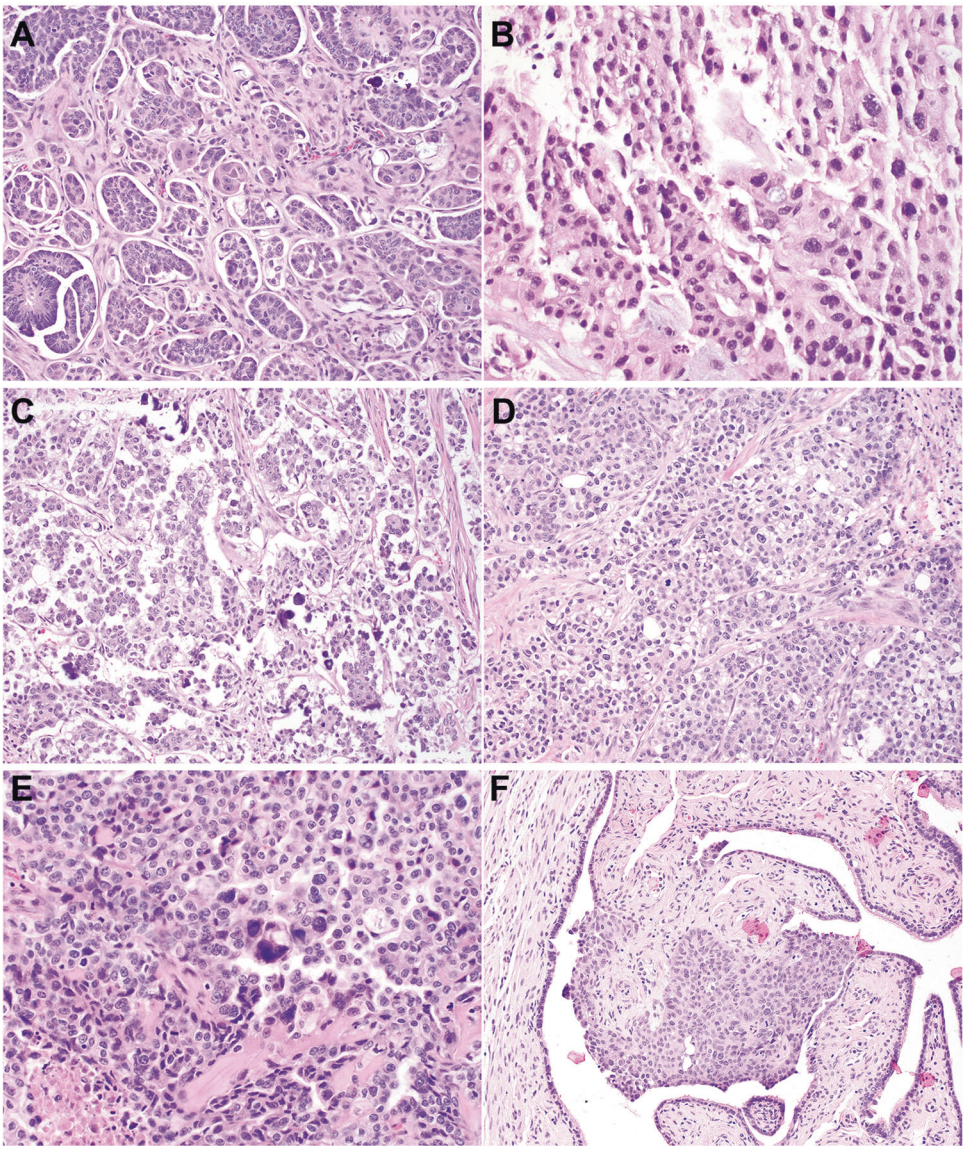


**Fig. 4 Morphologic spectrum of *TP53*-wildtype LGSC-like HGSCs. a** Case 2—Grade 2 nuclear features and micropapillary architecture (×200). **b** Case 4—High-grade carcinoma composed of solid sheets tumor cells with abortive gland formation, pleomorphic nuclei (Grade 3) and abundant eosinophilic cytoplasm (×400). Tumor was diffusely positive for WT1 and Pax8. **c**, **d** Case 8—Some areas resemble LGSC (**c** ×200), while other areas show increased nuclear pleomorphism and mitoses (**d** ×200). **e**, **f** Case 9—Grade 2 nuclear features, with scattered large, bizarre nuclei (**e** ×400) and exhibiting fallopian tube mucosal involvement (**f** ×200).

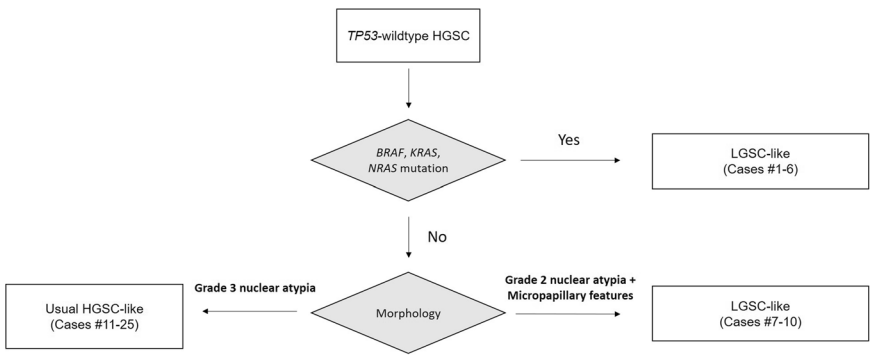


**Fig. 5** Flowchart indicating criteria for subclassification of *TP53*-wildtype HGSC.

outright). Within our cohort, 10 of 25 (40%) cases fit within the LGSC-like category (Cases 1–10; Fig. 4a–f). Of note, in Cases 2, 8, and 10, there were focal areas within the tumor, which taken in isolation, could be interpreted as low grade, though these were juxtaposed with a distinct high grade component. Cases 1, 2, 4, and 10 were also associated with a prior pathologic diagnosis of serous borderline tumor or LGSC.

The other major group is characterized by morphologic features of conventional HGSC ($n = 15$, 60%), henceforth

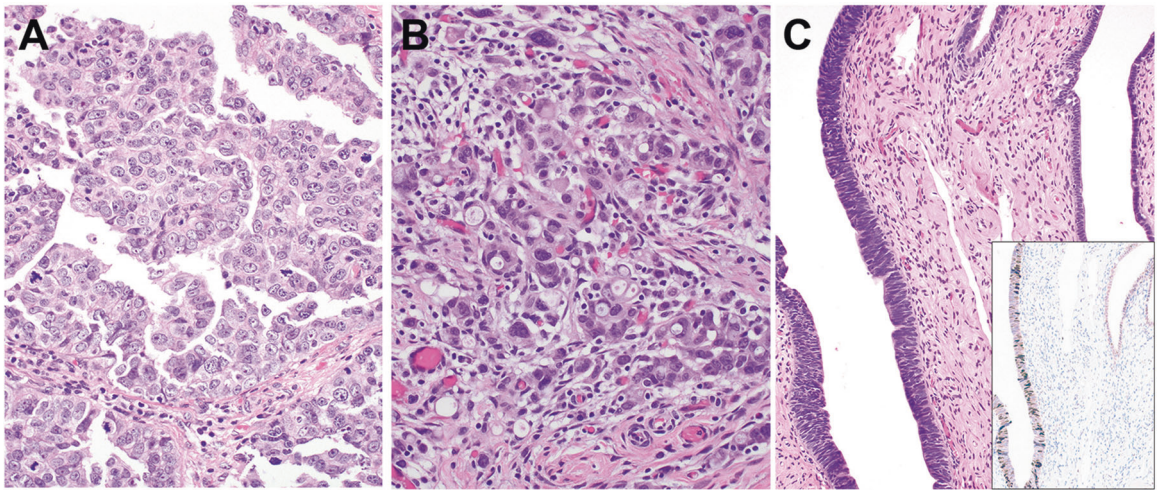


**Fig. 6** ***TP53*-wildtype usual HGSC-like tumors. a** Case 19 (×200). **b** Case 22, residual tumor post-neoadjuvant chemotherapy with prominent cytoplasmic vacuolation (×400; tumor associated with germline *APC* pathogenic variant). **c** Case 24—Fallopian tube with serous tubal intraepithelial carcinoma, (×200; inset: p53 immunostain shows wildtype expression pattern in serous tubal intraepithelial carcinoma).

designated as "usual HGSC-like" (Cases 11–25; Fig. 6a–c). Table 2 summarizes the clinicopathologic features of these designated tumor subgroups.

## Somatic driver gene mutations and copy number alterations

Targeted sequencing of known cancer genes confirmed the heterogeneity within the cohort (Fig. 3). The most frequent somatic mutations in the cohort of *TP53*-wildtype HGSCs involved genes implicated in RAS/MAPK signaling, specifically *KRAS*, *NRAS*, and *BRAF* ($n = 6$). While by definition, none of the tumors harbored mutations or homozygous deletions of *TP53*, loss-of-heterozygosity of this locus was observed in 7 (28%) cases. Since loss of heterozygosity did not associate with p53 immunohistochemical staining pattern or tumor subgroup, the biologic significance of this finding is unclear. The frequencies of somatic genetic alterations found in *TP53*-wildtype HGSCs relative to *TP53*-mutated HGSC within the MSK-IMPACT cohort ($n = 962$) are provided in Supplementary Table 2 for reference.

Amongst the LGSC-like HGSCs, of the 6 with mutations in *KRAS*, *BRAF,* or *NRAS* (Cases 1–6), 2 (Cases 2 and 3) showed Grade 2 nuclear atypia and micropapillary architecture. Cases 1 and 4 exhibited Grade 3 nuclear atypia, Case 5 cannot be assessed due to chemotherapy-related changes (though the pre-treatment specimen showed prominent micropapillary architecture), and Case 6 had Grade 2 nuclei, but was predominantly papillary, with only focal micropapillary architecture. It is worth mention that Case 4 was initially classified as high-grade carcinoma (not otherwise specified), due to its ambiguous morphology, characterized by solid sheets of tumor cells with abortive gland formation, abundant cytoplasm and pleomorphic nuclei (Fig. 4b). However, given the diffuse staining for WT1 and PAX8, prior serous borderline tumor, and presence of *NRAS* mutation, the features were considered compatible with an unusual form of HGSC that evolved from serous borderline tumor. Case 5 had *NRAS* and *EIF1AX* mutations, a combination characteristic of a subset of LGSCs, and therefore, was considered LGSC-like based on the genetic profile, despite the relatively non-specific morphology [16]. While Cases 7–9 lacked *RAS/RAF* mutations, they harbored loss-of-function genetic alterations of *NF1* or *NF2*, known to induce activation of MAPK signaling and have been reported in LGSC [7], as well as concurrent genetic features of HGSC, namely, *CCNE1* amplification (Case 9) and *BRCA2* mutations (Cases 7, 8). Case 10 did not have any gene alteration known to impact the MAPK pathway; however, it did harbor homozygous deletion of *CDKN2A* (encoding the p16 tumor suppressor), a finding that occurs more frequently in LGSC than HGSC [7]. Loss of *CDKN2A* was also observed in Case 8, by frameshift mutation, and Case 9, by homozygous deletion.

Within the group of usual HGSC-like tumors, amplification of *MDM2*, a known alternative mechanism for inactivation of p53, was detected in Cases 19 and 24. Other recurrent somatic genetic alterations seen exclusively in this group included loss-of-function of *RAD21* (Cases 16 and 20, by gene fusion), and *ARID1B* (Case 18 by gene fusion and Case 19 by frameshift mutation). RAD21 normally functions in homologous recombination-mediated repair of DNA double-strand breaks and chromosome segregation during mitosis [17], while ARID1B is a member of the SWI/SNF complex, previously reported to show concurrent loss with ARID1A in ovarian and endometrial de-differentiated carcinomas [18].

**Table 2** Subgroup comparisons of *TP53*-wildtype high-grade serous carcinomas.

| Feature | | LGSC-like | Usual HGSC-like | *p* Value |
|---|---|---|---|---|
| Prior SBT/LGSC | Yes | 4/10 (40%) | 0/15 (0%) | 0.017 |
| | No | 6/10 (60%) | 15/15 (100%) | |
| Nuclear atypia | Grade 2 | 7/9 (78%) | 0/10 (0%) | 0.0007 |
| | Grade 3 | 2/9 (22%) | 10/10 (100%) | |
| Micropapillary features | Yes | 7/9 (78%) | 3/10 (30%) | 0.07 |
| | No | 2/9 (22%) | 7/10 (70%) | |
| Mitotic rate | ≤12 | 4/9 (44%) | 2/9 (22%) | 0.62 |
| | >12 | 5/9 (56%) | 7/9 (78%) | |
| Fallopian tube mucosal lesion | STIC | 1/7 (14%) | 5/11 (46%) | 0.047[a] |
| | Mucosal involvement by carcinoma (no definitive STIC) | 2/7 (29%) | 5/11 (46%) | |
| | Negative for malignancy | 4/7 (57%) | 1/11 (8%) | |
| p53 expression | Wildtype | 7/9 (78%) | 4/14 (29%) | 0.036[b] |
| | Diffuse | 1/9 (11%) | 1/14 (7%) | |
| | Null | 1/9 (11%) | 5/14 (36%) | |
| | Equivocal (Wt vs null) | 0/9 (0%) | 4/14 (29%) | |
| *KRAS*, *BRAF*, or *NRAS* mutation | Yes | 6/10 (60%) | 0/15 (0%) | 0.0012 |
| | No | 4/10 (40%) | 15/15 (100%) | |

*SBT* serous borderline tumor, *LGSC* low-grade serous carcinoma, *HGSC* high-grade serous carcinoma, *STIC* serous tubal intraepithelial carcinoma.

[a]Comparison of STIC and mucosal carcinoma as a group versus negative for malignancy.

[b]Comparison of wildtype versus other (null/diffuse/equivocal) staining pattern.

## Global genomic alterations

For cases with adequate tumor purity, the extent of genomic abnormalities of *TP53*-wildtype HGSC was compared to randomly selected LGSCs ($n = 58$) and *TP53*-mutated HGSCs ($n = 109$) from the institutional MSK-IMPACT database. While the fraction of genome altered by copy number gains or losses spanned a broad range for each group, overall, *TP53*-mutated HGSCs exhibited a significantly higher fraction of genome altered than LGSCs and *TP53*-wildtype HGSCs (Fig. 7a). A more direct measure of DNA damage is the rate of intrachromosomal breakpoints, represented by the breakpoint instability index. Despite some degree of overlap, intrachromosomal breakpoints were more extensive in the *TP53*-mutated HGSC genome relative to LGSC, while *TP53*-wildtype HGSC was situated in between [breakpoint instability index, median (IQR): for LGSC, 14 (3–42); for *TP53*-wildtype HGSC, 73 (37–150); for *TP53*-mutated HGSC, 188 (125–292); Fig. 7b]. Tumor mutational burden was low overall. While statistically significant differences were observed between groups for this parameter, these were of low magnitude, and thus, the clinical or biologic significance of this finding is unclear (Fig. 7c).

In subgroup analyses, most LGSC-like HGSCs had higher levels of chromosomal instability than typically seen in LGSC (6/8 cases above the LGSC median values for both parameters, fraction of genome altered and breakpoint instability index). No statistically significant differences were observed when comparing this group with usual HGSC-like tumors (fraction of genome altered, $p = 0.75$; breakpoint instability index, $p = 0.30$); however, the sample size may be too small for meaningful subgroup analysis. Of note, Cases 7, 8, and 9, which showed Grade 2 nuclear atypia and micropapillary features, along with mixed genetic features of both LGSC and HGSC (namely, alterations of *NF1/2*, *CDKN2A*, *BRCA2* and *CCNE1*), had frequent intrachromosomal breakpoints (breakpoint instability index above the *TP53*-wildtype HGSC median).

## Germline mutations

Nine patients harbored germline pathogenic variants in known cancer predisposition genes, including genes involved in the homologous recombination pathway of DNA repair (*BRCA1*, *BRCA2*, or *PALB2*) in 6 patients, all of whom presented with usual HGSC-like tumors (Fig. 3). As previously stated, 2 LGSC-like HGSCs (Cases 7 and 8) harbored somatic *BRCA2* mutations.

The remaining germline variants involved *APC* (I1307K in Cases 17 and 22, both usual HGSC-like) and *MUTYH* (G382D, Case 4, LGSC-like). *APC* I1307K is a low penetrance variant that is known to confer a slight increased risk of colorectal cancer, while bi-allelic *MUTYH* variants are causative of an autosomal recessive polyposis syndrome [19]. While germline *APC* and *MUTYH* variants have not been associated with a predisposition to HGSC, we note the

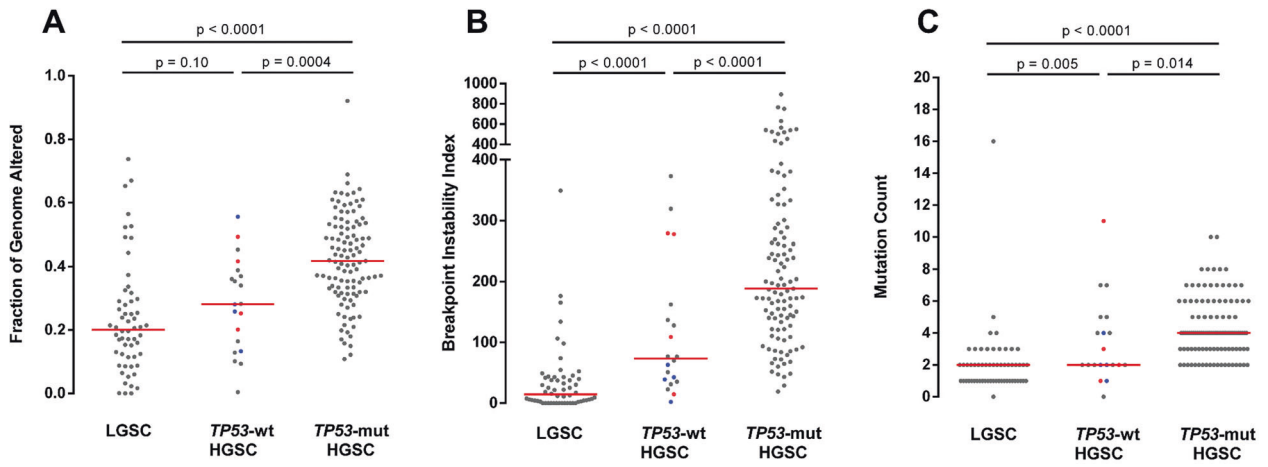


**Fig. 7 Genomic instability of *TP53*-wildtype HGSC relative to LGSC and *TP53*-mutated HGSC. a** Fraction of genome altered by copy number gains and losses. **b** Breakpoint instability index, a measure of the number of intrachromosomal breakpoints across the genome. **c** Total number of somatic mutations. Colored dots indicate LGSC-like *TP53*-wildtype HGSCs: Blue—with *KRAS*, *BRAF* or *NRAS* mutation; red—without *KRAS*, *BRAF* or *NRAS* mutation. Red horizontal line designates the median. Statistical comparisons performed using the Mann–Whitney test, two-tailed.

unusual histomorphology of Case 4 (previously described under the section, *Somatic genetic alterations*, Fig. 4b) and Case 22 (Fig. 6b). Case 22 was characterized by prominent intracytoplasmic mucin vacuoles, which imparted a microcystic appearance. While this may have been related to neoadjuvant chemotherapy, cells with similar morphology were focally seen in the other patient with *APC* mutation (Case 17), who did not receive chemotherapy. Of note, both cases with diffuse p53 staining in *TP53*-wildtype HGSC cohort were observed in the context of germline *APC* or *MUTYH* variants.

### Fallopian tube mucosal involvement

Slides of fallopian tube were available for 18 *TP53*-wildtype HGSCs and evaluated for mucosal-based lesions. In 6 cases, there was definitive evidence of STIC, either present alone (Cases 19, 22, 24) or adjacent to areas of carcinoma, the latter characterized by papillary or invasive growth or a mass-forming lesion (Cases 9, 12, 17). In another 7 cases, there was involvement of tubal mucosa by carcinoma, but due to its extensive nature, it was unclear whether this represented in-situ disease versus metastatic colonization. Subgroup comparison of LGSC-like with usual HGSC-like tumors revealed a significantly higher frequency of tubal mucosal involvement in the latter [3/7 (43%) versus 10/11 (91%), $p = 0.047$; of these, STIC represented 1 and 5 cases, respectively, Figs. 4f and 6c].

### Immunohistochemical staining for p53

Immunohistochemical staining for p53 in 23 *TP53*-wildtype HGSCs demonstrated a definitive wildtype expression pattern in 11 (48%), diffuse strong staining in 2 (9%), complete loss of expression in 6 (26%) and focal weak nuclear staining limited to rare tumor cells in 4 (17%), which was interpreted as equivocal for wildtype versus null pattern (Fig. 8). None of the cases showed the cytoplasmic (mutant-type) staining pattern.

The distribution of p53 staining patterns was significantly different in LGSC-like compared to usual HGSC-like tumors. Most LGSC-like tumors (7/9, 78%) showed a wildtype expression pattern, compared to 4 of 14 (29%) usual HGSC-like tumors ($p = 0.036$, Table 2). Of note, all cases with aberrant immunohistochemical p53 staining passed quality control criteria for molecular analysis (with estimated tumor cellularity >20%, average variant allele frequency >5%), and thus the discordances are unlikely due to *TP53* mutations missed by sequencing.

## Discussion

*TP53* mutation has been reported in virtually all HGSCs, and even in early tubal precursor lesions, consistent with this being an important driver in the pathogenesis of the disease. Despite this well-established dogma, controversy remains over the existence of rare *TP53*-wildtype HGSC. A few cases of HGSCs lacking *TP53* mutation have been reported as anomalies within larger cohorts, occurring at frequencies ranging from 1–4% [6, 20–22]. One group analyzed data from the TCGA ovarian cancer study and reported 15 HGSCs lacking a *TP53* mutation [22], however, subsequent pathology review of these cases by an independent group of gynecologic pathologists concluded that most were other ovarian carcinoma subtypes (LGSC,

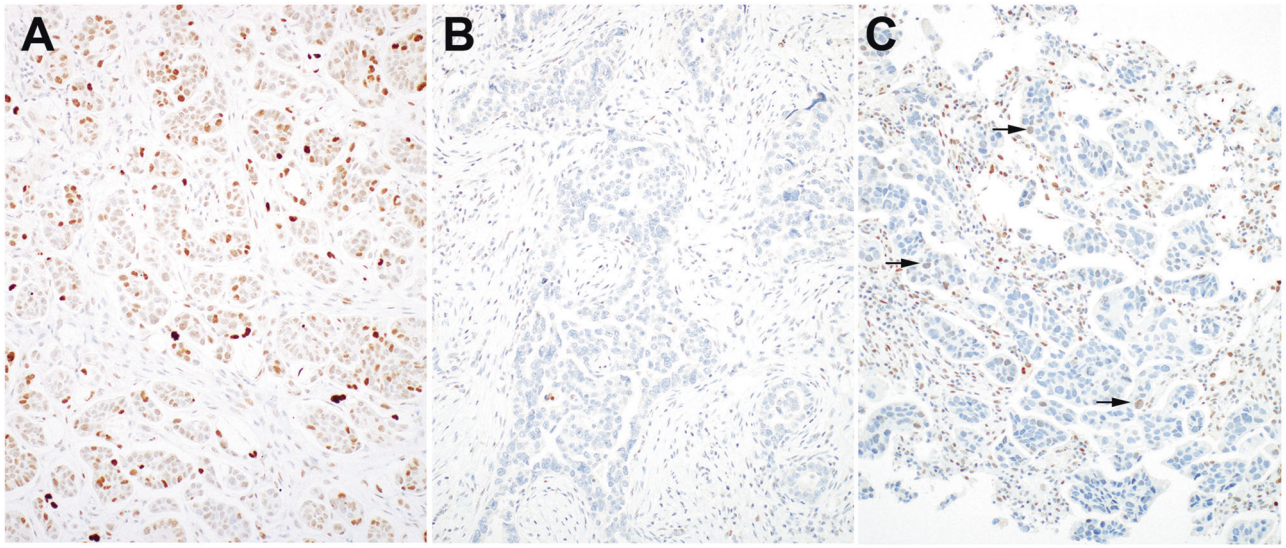


**Fig. 8 Immunohistochemical staining pattern of p53 in *TP53*-wildtype HGSCs. a** Wildtype expression pattern (Case 2). **b** Null pattern, characterized by complete absence of staining (Case 16). **c** Equivocal staining (wildtype versus null pattern; Case 13), with rare weakly positive cells (arrows). All photomicrographs at ×200 magnification.

endometrioid or clear cell) that were misclassified as HGSC [6]. Only 2 were interpreted as HGSC by all observers: one had a homozygous deletion of the *TP53* gene and the other had features suggesting evolution from LGSC.

To gain further insight into HGSCs that lack *TP53* alterations, we conducted a rigorous molecular and histopathologic review of HGSCs that underwent molecular profiling by MSK-IMPACT. The present series represents the largest cohort of such patients reported in the literature to date, with comprehensive clinicopathologic, immunophenotypic and molecular genetic characterization. Importantly, we excluded cases with low tumor purity, for which a mutation-negative result was likely artefactual, and re-reviewed the sequencing reads for low-frequency or unusual allelic variants (i.e., large deletions, synonymous or intronic mutations affecting splicing), ensuring that all cases are truly *TP53*-wildtype.

In contrast to the study by Vang et al., in which observers were aware of the *TP53*-wildtype status of the cases, in our present study, a mix of *TP53*-wildtype and *TP53*-mutated HGSCs were reviewed by observers blinded to mutation status. In addition to avoiding potential bias, this approach allowed us to compare the morphologic features of *TP53*-wildtype and *TP53*-mutated HGSCs.

The most striking result is the finding of a disproportionate enrichment of cases with moderate-to-severe nuclear atypia and exhibiting micropapillary features amongst *TP53*-wildtype HGSCs. A subset of these also harbored driver mutations in *KRAS*, *NRAS,* or *BRAF*, which have been reported in up to 60% of serous borderline tumors or LGSCs but are exceedingly rare in HGSC. High-grade transformation of serous borderline tumor or LGSC is a rare, but recognized, phenomenon, and could occur without acquiring a *TP53* mutation [9–12]. We note that not all tumors with *RAS/RAF* mutations in our cohort showed Grade 2 nuclear atypia and micropapillary features, and conversely, tumors with highly suggestive morphology did not necessarily harbor the characteristic mutations. Since up to 40% of LGSCs are wildtype for *RAS/RAF* mutation, this finding does not necessarily discount the possibility of low-grade serous origin. Given only partial overlap in cases with morphologic and genetic features characteristic of low-grade serous neoplasia, we considered either presence of *RAS/RAF* mutation or the combination of cytologic and architectural features as definitional of LGSC-like HGSC. Most of these tumors showed higher levels of chromosomal instability than typically observed in LGSC, but lower than *TP53*-mutated HGSC. Some exhibited other features of HGSC, including high mitotic index, association with STIC or fallopian tube mucosal involvement, and genetic alterations of *BRCA2* or *CCNE1*. While it is likely that a proportion of LGSC-like HGSCs evolved from a low-grade serous tumor, the possibility of de novo histogenesis (potentially even from a tubal precursor) cannot be excluded.

Our findings build upon prior morphologic studies of so-called "intermediate" or "indeterminate" grade serous carcinomas. An earlier study from the Johns Hopkins group suggested that these were equivalent to conventional HGSC, since virtually all the tumors in their study had *TP53* mutations and lacked *BRAF* or *KRAS* mutations [23]. However, in recent work by Zarei et al., the majority of their "indeterminate" grade tumors lacked *TP53* mutations and the authors proposed that at least a subset presumably developed from pre-existing LGSC [24]. The contrasting

results between studies highlight the intrinsic subjectivity in the assessment of nuclear atypia for these borderline cases. Despite the different methodological approach employed by Zarei et al., who selected cases based on morphology, and our present study, in which cases were selected based on the *TP53* mutation-negative molecular result, included within our cohort are examples of the same entity they describe as "indeterminate grade serous carcinoma." Of note, out of 171 HGSCs, Kobel et al. also identified 2 without *TP53*-mutation, which were positive for WT1 by immunohistochemistry, had moderate nuclear atypia, and therefore, likely also fit into this category [21].

What about the other *TP53*-wildtype tumors? These were otherwise similar to conventional HGSCs, and many were associated with either STIC or involvement of tubal mucosa by carcinoma, as commonly observed with this histotype. Despite intact *TP53* at the genetic level, the majority showed decreased or loss of p53 protein expression, in contrast to the LGSC-like HGSCs, which tended to show a clear wildtype immunostaining pattern. Two of these usual HGSC-like tumors demonstrated amplification of *MDM2*, an oncogene that targets p53 for degradation by the proteasome [25], akin to a previously reported case of *MDM2*-amplified, *TP53*-mutation-negative HGSC [20]. These findings suggest alternative mechanisms for p53 dysfunction in HGSCs that lack *TP53* genetic alterations, either by silencing expression (potentially mediated by some epigenetic mechanism), MDM2-mediated degradation, or some other unknown molecular mechanism that enables cells to bypass the tumor suppressive actions of p53.

Germline mutations associated with *TP53*-mutated HGSC include genes implicated in hereditary breast and ovarian cancer syndrome, namely, *BRCA1/2* and *PALB2*, which supported the HGSC diagnosis. The biologic significance of germline colorectal polyposis-associated *MUTYH* and *APC* variants identified in three cases is uncertain. MUTYH-associated polyposis is an autosomal recessive condition that has been associated with increased risk of ovarian cancer [26]; however, the predisposition syndrome requires bi-allelic mutations, while Case 4 in our cohort was a heterozygous carrier. The *APC* I1307K mutation has a prevalence of ~6% in the Ashkenazi Jewish population, and studies to date have concluded its association with ovarian cancer to be coincidental [27, 28]. However, the interesting finding that the *TP53*-wildtype HGSCs with diffuse p53 staining were of unusual morphology and from patients with *MUTYH* or *APC* germline variants raises the possibility that there may be some unknown molecular connection specific to these rare tumors.

The identification of rare tumors with aberrant p53 immunohistochemical staining pattern despite lacking *TP53* genetic alterations ($n = 8$) contrasts with a prior study demonstrating 100% of ovarian HGSC with aberrant immunohistochemical staining harbored underlying *TP53* genetic alterations, while only 4% of tumors with a wildtype staining pattern were associated with unusual loss-of-function mutations [21]. We believe our cases represent rare exceptions to the rule and unlikely attributed to false-negative mutational analysis, for the following reasons: (1) we used a hybridization-capture sequencing approach, which has higher sensitivity in detecting low-frequency variants, compared to the amplicon-sequencing approach used in the prior study; (2) sensitivity is further improved by sequencing matched tumor and normal samples for each case; (3) the assay covers the entirety of *TP53* exons, as well as flanking intronic sequences; (4) All of the cases met strict quality control metrics including DNA and library yield, coverage, fragment size, GC bias, and minimum tumor purity requirement. Of note, we excluded low-cellularity cases with aberrant immunostaining, as these were recognized as false-negative molecular results, and excluded additional cases with unusual variants, upon manual re-review of sequencing reads. In our final cohort, the discordant immunohistochemical staining in the 8 cases therefore suggests alternative (i.e. epigenetic) mechanisms affecting expression of p53, as discussed earlier. In this context, our findings should not be viewed as failure of p53 immunohistochemical staining to predict mutation status.

Given the small sample size and limited clinical follow-up for most cases, the study is underpowered for prognostic stratification. Preliminary exploratory analyses suggest a possible trend toward improved clinical outcome of *TP53*-wildtype compared to conventional *TP53*-mutated HGSC (data not shown); however, at the time of writing, it is too early to draw meaningful conclusions from the clinical outcome data. We plan to address this issue in a future case-control study when the data matures.

In conclusion, we provide compelling histomorphologic, immunophenotypic and molecular genetic evidence supporting the existence of *TP53*-wildtype HGSCs, which are rare tumors that make up 2.5% of all tubo-ovarian HGSCs. Around 40% demonstrate mixed morphologic and/or genetic features of both LGSC and HGSC and presumably evolved from a low-grade serous tumor. The remainder are morphologically indistinguishable from *TP53*-mutated HGSC and often exhibit loss of p53 expression despite intact *TP53* at the genetic level. With the increasing role of tumor molecular profiling in clinical decision-making, our reported findings continue to highlight the primary importance of traditional histomorphologic criteria for the diagnosis of HGSC. Indeed, while demonstration of an underlying *TP53* genetic alteration would serve as confirmatory evidence, the unusual scenario of a negative molecular result should not automatically discredit the original pathologic diagnosis.

**Acknowledgements** We thank Dr. Lora Hedrick Ellenson for her thoughtful comments on the manuscript.

## Compliance with ethical standards

**Conflict of interest** The authors declare that they have no conflict of interest.

**Publisher's note** Springer Nature remains neutral with regard to jurisdictional claims in published maps and institutional affiliations.

## References

1. Kurman RJ, Shih IM. The dualistic model of ovarian carcinogenesis: revisited, revised, and expanded. Am J Pathol. 2016;186:733–47.
2. Labidi-Galy SI, Papp E, Hallberg D, Niknafs N, Adleff V, Noe M, et al. High grade serous ovarian carcinomas originate in the fallopian tube. Nat Commun. 2017;8:1093.
3. Carlson JW, Miron A, Jarboe EA, Parast MM, Hirsch MS, Lee Y, et al. Serous tubal intraepithelial carcinoma: its potential role in primary peritoneal serous carcinoma and serous cancer prevention. J Clin Oncol. 2008;26:4160–5.
4. Seidman JD, Bell DA, Crum CP, filler O. Tumours of the ovary: epithelial tumours—serous tumours., In: Kurman RJ, Carcangiu ML, Herrington CS, filler O, editors. WHO Classification of Tumours of Female Reproductive Organs. Lyon: IARC Press; 2014. p. 17–24.
5. The Cancer Genome Atlas Research Network. Integrated genomic analyses of ovarian carcinoma. Nature. 2011;474:609–15.
6. Vang R, Levine DA, Soslow RA, Zaloudek C, Shih Ie M, Kurman RJ. Molecular alterations of TP53 are a defining feature of ovarian high-grade serous carcinoma: a rereview of cases lacking TP53 mutations in the Cancer Genome Atlas Ovarian Study. Int J Gynecol Pathol. 2016;35:48–55.
7. Hunter SM, Anglesio MS, Ryland GL, Sharma R, Chiew YE, Rowley SM, et al. Molecular profiling of low grade serous ovarian tumours identifies novel candidate driver genes. Oncotarget. 2015;6:37663–77.
8. Malpica A, Deavers MT, Lu K, Bodurka DC, Atkinson EN, Gershenson DM, et al. Grading ovarian serous carcinoma using a two-tier system. Am J Surg Pathol. 2004;28:496–504.
9. Murali R, Selenica P, Brown DN, Cheetham RK, Chandramohan R, Claros NL, et al. Somatic genetic alterations in synchronous and metachronous low-grade serous tumours and high-grade carcinomas of the adnexa. Histopathology. 2019;74:638–50.
10. Chui MH, Xing D, Zeppernick F, Wang ZQ, Hannibal CG, Frederiksen K, et al. Clinicopathologic and molecular features of paired cases of metachronous ovarian serous borderline tumor and subsequent serous carcinoma. Am J Surg Pathol. 2019;43:1462–72.
11. Garg K, Park KJ, Soslow RA. Low-grade serous neoplasms of the ovary with transformation to high-grade carcinomas: a report of 3 cases. Int J Gynecol Pathol. 2012;31:423–8.
12. Boyd C, McCluggage WG. Low-grade ovarian serous neoplasms (low-grade serous carcinoma and serous borderline tumor) associated with high-grade serous carcinoma or undifferentiated carcinoma: report of a series of cases of an unusual phenomenon. Am J Surg Pathol. 2012;36:368–75.
13. Parker RL, Clement PB, Chercover DJ, Sornarajah T, Gilks CB. Early recurrence of ovarian serous borderline tumor as high-grade carcinoma: a report of two cases. Int J Gynecol Pathol. 2004;23:265–72.
14. Cheng DT, Mitchell TN, Zehir A, Shah RH, Benayed R, Syed A, et al. Memorial Sloan Kettering-Integrated Mutation Profiling of Actionable Cancer Targets (MSK-IMPACT): a hybridization capture-based next-generation sequencing clinical assay for solid tumor molecular oncology. J Mol Diagn. 2015;17:251–64.
15. Zhang NR, Siegmund DO. A modified Bayes information criterion with applications to the analysis of comparative genomic hybridization data. Biometrics. 2007;63:22–32.
16. Etemadmoghadam D, Azar WJ, Lei Y, Moujaber T, Garsed DW, Kennedy CJ, et al. EIF1AX and NRAS mutations co-occur and cooperate in low-grade serous ovarian carcinomas. Cancer Res. 2017;77:4268–78.
17. Xu H, Balakrishnan K, Malaterre J, Beasley M, Yan Y, Essers J, et al. Rad21-cohesin haploinsufficiency impedes DNA repair and enhances gastrointestinal radiosensitivity in mice. PLoS ONE. 2010;5:e12112.
18. Coatham M, Li X, Karnezis AN, Hoang LN, Tessier-Cloutier B, Meng B, et al. Concurrent ARID1A and ARID1B inactivation in endometrial and ovarian dedifferentiated carcinomas. Mod Pathol. 2016;29:1586–93.
19. Leoz ML, Carballal S, Moreira L, Ocana T, Balaguer F. The genetic basis of familial adenomatous polyposis and its implications for clinical practice and risk management. Appl Clin Genet. 2015;8:95–107.
20. Ahmed AA, Etemadmoghadam D, Temple J, Lynch AG, Riad M, Sharma R, et al. Driver mutations in TP53 are ubiquitous in high grade serous carcinoma of the ovary. J Pathol. 2010;221:49–56.
21. Kobel M, Piskorz AM, Lee S, Lui S, LePage C, Marass F, et al. Optimized p53 immunohistochemistry is an accurate predictor of TP53 mutation in ovarian carcinoma. J Pathol Clin Res. 2016;2:247–58.
22. Wong KK, Izaguirre DI, Kwan SY, King ER, Deavers MT, Sood AK, et al. Poor survival with wild-type TP53 ovarian cancer? Gynecol Oncol. 2013;130:565–9.
23. Ayhan A, Kurman RJ, Yemelyanova A, Vang R, Logani S, Seidman JD, et al. Defining the cut point between low-grade and high-grade ovarian serous carcinomas: a clinicopathologic and molecular genetic analysis. Am J Surg Pathol. 2009;33:1220–4.
24. Zarei S, Wang Y, Jenkins SM, Voss JS, Kerr SE, Bell DA. Clinicopathologic, immunohistochemical, and molecular characteristics of ovarian serous carcinoma with mixed morphologic features of high-grade and low-grade serous carcinoma. Am J Surg Pathol. 2020;44:316–28.
25. Haupt Y, Maya R, Kazaz A, Oren M. Mdm2 promotes the rapid degradation of p53. Nature. 1997;387:296–9.
26. Vogt S, Jones N, Christian D, Engel C, Nielsen M, Kaufmann A, et al. Expanded extracolonic tumor spectrum in MUTYH-associated polyposis. Gastroenterology. 2009;137:e1–10.
27. Gershoni-Baruch R, Patael Y, Dagan, Figer A, Kasinetz L, Kadouri E, et al. Association of the I1307K APC mutation with hereditary and sporadic breast/ovarian cancer: more questions than answers. Br J Cancer. 2000;83:153–5.
28. Maresco DL, Arnold PH, Sonoda Y, Federici MG, Bogomolniy F, Rhei E, et al. The APC I1307K allele and BRCA-associated ovarian cancer risk. Am J Hum Genet. 1999;64:1228–30.